Thirteenth USA/Europe Air Traffic Management Research and Development Seminar (ATM2019)

Model Predictive Control Approach to Storm Avoidance for Multiple Aircraft

Dinesh B. Seenivasan, Alberto Olivares and Ernesto Staffetti
Universidad Rey Juan Carlos
Fuenlabrada, Madrid, Spain
seenivasan.dinesh@urjc.es, alberto.olivares@urjc.es, ernesto.staffetti@urjc.es

***Abstract*—This paper studies the trajectory generation problem for multiple aircraft in converging and intersecting arrival routes in the presence of a multi-cell storm in development. Storm avoidance constraints are enforced by approximating the cells of the storm as moving and size-changing ellipsoids. The problem is solved using nonlinear model predictive control based on hybrid optimal control with logical constraints in disjunctive form. The evolution of the storm is tackled using the nonlinear model predictive control scheme, which iteratively re-plans the trajectories as a new estimation of the state of the storm is available. Logical constraints in disjunctive form arise in modelling passage through waypoints and storm avoidance constraints. An embedding approach is employed to transform these logical constraints in disjunctive form into inequality and equality constraints which involve only continuous auxiliary variables. In this way, the hybrid optimal control problem is converted into a smooth optimal control problem, thereby reducing the computational complexity of finding the solution.**

***Index Terms*—4D Trajectory Generation, Storm Avoidance, Air Traffic Management, Hybrid Optimal Control, Nonlinear Model Predictive Control.**

I. Introduction

In this paper, the trajectory generation problem is studied for multiple aircraft in converging and intersecting arrival routes in the presence of a multi-cell storm in development. Thus, besides storm avoidance constraints, operational constraints are also taken into account and a Nonlinear Model Predictive Control (NMPC) scheme based on hybrid optimal control with logical constraints in disjunctive form has been employed.

Forecasting with precision the birth and evolution of convective weather phenomena at pre-tactical timescales (1-3 hours before departure) is not an easy task, which makes it hard for flight dispatchers to plan flights to avoid them. Although some meteorological conditions, which are required for storm formation, can be forecasted in advance, the specific location and timing of convective storms is difficult to determine. As a consequence, both storm forecasting and avoidance take place at short timescales, mainly at execution stage, that is, during flight. Storm prediction is usually given in the form of deterministic nowcast such as the Rapidly Developing Thunderstorms (RDT), which is one of the meteorological products of the Satellite Application Facility on support to Nowcasting and Very Short-Range Forecasting (NWCSAF) consortium[1]. The RDT system characterizes thunderstorm activity providing images every 15 minutes with a horizontal resolution of 3 km. It identifies convective cells and describes them as polygons on a latitude-longitude map. It contains the identified convective storms, along with some of their features such as perimeter, direction of motion and speed and the cloud top pressure (the latter, needed to characterize the height of the storm). It also provides a description of the phase of the convective cell: triggering, triggering from split, growing, mature and decaying. These parameters are then employed to predict the evolution of the storm over a short time horizon and corrected as soon as a new observation becomes available. Thus, the RTD-based forecast can be regarded as a moving horizon estimation, for which a well-suited scheme for trajectory generation is the Model Predictive Control (MPC) scheme [1].

In this NMPC setting, the optimal trajectories for the aircraft are calculated taking into account the prediction of the future behaviour of the storm over a certain time horizon, based on measurements obtained at a certain time instant. Due to disturbances and modelling prediction errors, the behaviour of the storm will be different from the predicted behaviour and the trajectories of the aircraft will deviate from the planned trajectories. In order to incorporate some feedback mechanism to correct these mismatches, the planned trajectories will be flown in open-loop until the next prediction of the storm becomes available. Then, the trajectory planning problem is solved again in a receding spatial and temporal horizon. For this reason, this control paradigm is also referred to as moving horizon control or receding horizon control. The presence of a feedback mechanism in this trajectory planning scheme, makes it substantially different from the open-loop trajectory planning methods and therefore, it has been herein called trajectory generation.

This study can be classified into the category of Continuous Descent Operations (CDO) [2]. During CDO, aircraft descend from the cruise altitude to the final approach fix at or near idle thrust without level segments at low altitude, minimizing the need for high thrust levels to remain at a constant altitude

This work has been partially supported by the grants TRA2013-47619-C2-2-R and TRA2017-91203-EXP of the Spanish Government.

[1] http://www.nwcsaf.org/

and reducing the environmental impact. Actually, the term CDO makes reference to the different techniques to maximize operational efficiency and, at the same time, fulfilling local air space requirements and constraints. These operations are known as Continuous Descent Arrivals, Optimized Profile Descents (OPDs), Tailored Arrivals, 3D Path Arrival Management, and Continuous Descent Approaches (CDA). In particular, an OPD is a descent profile normally associated with a Standard Terminal Arrival Route (STAR) and designed to allow maximum use of a CDO. Planning CDOs is one of the functions of the so called Arrival Managers (AMANs) whose purpose is to ensure an optimal sequencing and spacing of arrival traffic [3]. In this work, the problem of optimal sequencing of arrival traffic will be studied taking into account a multi-cell storm in development in the relevant airspace.

In most of the previous approaches to optimal aircraft trajectory planning in the presence of storms in development [4]–[8], a cell discretisation of the 3D or 4D space in which the problem is represented is performed. In these approaches, the problem is often studied in the en-route portion of the flight and the model of the aircraft is oversimplified. In general, a kinematic model of a unicycle with upper bounds on the turning rate is used to represent aircraft. This implies that the actual performance of the aircraft involved is not taken into account and this fact does not guarantee the dynamic feasibility of the resulting trajectories. Moreover, the solution method is based on a discrete search, which represents a further approximation of the problem whose nature is indeed continuous.

This paper is structured as follows. In Sec. II, the general optimal control problem for multiple dynamical systems is stated and the closed-loop NMPC approach based on open-loop direct collocation for its resolution is described. In Sec. III, the aircraft equations of motion and the flight envelope constraints are stated. In Sec. IV, the general approach to model logical constraints is presented, which is then particularized to model storm avoidance constraints and waypoint constraints. In Sec. V, the results of the application of the proposed method to solve a trajectory generation problem for multiple aircraft with logical constraints in disjunctive form are reported and discussed. Finally, in Sec. VI, some conclusions are drawn.

II. Optimal Control Approach

A. Nonlinear Model Predictive Control

As mentioned above, the aircraft trajectory generation problem considered in this paper has been tackled using a NMPC approach, which is a well-known technique that provides optimal feedback control of the studied dynamical system. In our NMPC setting, a finite horizon open-loop optimal control problem (see Sect II-B) at each time step is solved. Then, starting from the reached state, only the first control input of the optimal sequence is implemented. This strategy is repeated turning the open-loop path planning into a feedback control scheme. In this way, within each iteration, a locally optimal segment of trajectory moving towards the target is computed, obtaining a sequence of short trajectories, thus reducing the computational load.

B. Open-Loop Optimal Control

The multi-aircraft open-loop flight-planning problem considered in this work can be regarded as a multi-trajectory optimization problem, in which the motion of each aircraft has been modeled as a differential-algebraic dynamic system

$$\Sigma^p = \{f^p : \mathcal{X}^p \times \mathcal{U}^p \times \mathbb{R}^{n_{sp}} \to \mathbb{R}^{n_{xp}},\ g^p : \mathcal{X}^p \times \mathcal{U}^p \times \mathbb{R}^{n_{sp}} \to \mathbb{R}^{n_{zp}}\},$$

for $p = 1, 2, \ldots, N_p$, where f^p describes the right-hand side of the differential equation

$$\dot{x}^p(t) = f^p(x^p(t), u^p(t), s^p)$$

and g^p describes the algebraic constraints

$$0 = g^p(x^p(t), u^p(t), s^p),$$

where $\mathcal{X}^p \subseteq \mathbb{R}^{n_x^p}$ and $\mathcal{U}^p \subseteq \mathbb{R}^{n_u^p}$ are the state and control sets, respectively, $x^p(t) \in \mathbb{R}^{n_x^p}$ is a n_x^p-dimensional state variable, $u^p(t) \in \mathbb{R}^{n_u^p}$ is a n_u^p-dimensional control input, and $s^p \in \mathbb{R}^{n_s^p}$ is a vector of parameters.

Since this multi-aircraft flight-planning problem also involves operative performances and flight envelope conditions for multiple aircraft, as well as the optimization of a specified performance index, the multi-trajectory optimization problem can be formulated as an OCP of a set of dynamic systems in which the goal is to find the trajectories and the corresponding control inputs that steer the states of the systems between two configurations, satisfying a set of constraints on the state and/or control variables while minimizing an objective functional.

Therefore, the open-loop optimal control problem considered in this work can be stated as follows:

$$\min\ J(x(t), u(t), s, t) = \sum_{p=1}^{N_p} \Phi(t_F^p, x^p(t_F^p)) + \sum_{p=1}^{N_p} \int_{t_I^p}^{t_F^p} L^p(x^p(t), u^p(t), s^p, t)dt, \quad \text{(1a)}$$

subject to:

$$\dot{x}(t) = f(x(t), u(t), s, t), \quad \text{(1b)}$$

$$0 = g(x(t), u(t), s, t), \quad \text{(1c)}$$

$$\phi_l \leq \phi(x(t), u(t), s, t) \leq \phi_u, \quad \text{(1d)}$$

$$x(t_I) = x_I, \quad \text{(1e)}$$

$$\psi(x(t_F)) = 0, \quad \text{(1f)}$$

where

$$x = [x^1, x^2, \ldots, x^{N_p}]^T, u = [u^1, u^2, \ldots, u^{N_p}]^T,$$
$$s = [s^1, s^2, \ldots, s^{N_p}]^T,$$

and t_F^p denote de final time for aircraft $p = 1, 2, \ldots, N_p$. The objective function

$$J : \mathbb{R}^{n_x} \times \mathbb{R}^{n_u} \times \mathbb{R}^{n_s} \times [t_I, t_F] \to \mathbb{R}$$

is given in Bolza form. It is expressed as a combination of a Mayer term

$$\sum_{p=1}^{N_p} \Phi(t_F^p, x^p(t_F^p))$$

and a Lagrange term

$$\sum_{p=1}^{N_p} \int_{t_I^p}^{t_F^p} L^p(x^p(t), u^p(t), s^p, t)dt.$$

Functions

$$\Phi^p : [t_I^p, t_F^p] \times \mathbb{R}^{n_{x^p}} \to \mathbb{R}$$

and

$$L^p : \mathbb{R}^{n_{x^p}} \times \mathbb{R}^{n_{u^p}} \times \mathbb{R}^{n_{z^p}} \times [t_I^p, t_F^p] \to \mathbb{R}$$

are assumed to be twice differentiable. Function f is assumed to be piecewise Lipschitz continuous within the time interval $[t_I, t_F]$, and the derivative of the algebraic right-hand side function g with respect to z, that is,

$$\frac{\partial g}{\partial z} \in \mathbb{R}^{n_z \times n_z}$$

is assumed to be regular within the time interval $[t_I, t_F]$. Vector $x_I \in \mathbb{R}^{n_x}$ represents the initial conditions given at the initial time t_I and function

$$\psi : \mathbb{R}^{n_x} \to \mathbb{R}^{n_\psi}$$

provides the terminal conditions at the final time t_F, and it is assumed to be twice differentiable. The system must also satisfy algebraic path constraints within the time interval $[t_I, t_F]$ given by the vector function

$$\phi : \mathbb{R}^{n_x} \times \mathbb{R}^{n_u} \times \mathbb{R}^{n_z} \to \mathbb{R}^{n_\phi},$$

with lower bound $\phi_l \in \mathbb{R}^{n_\phi}$ and upper bound $\phi_u \in \mathbb{R}^{n_\phi}$. Function ϕ is assumed to be twice differentiable.

In the objective function (1a), the Lagrange term represents a running cost, whereas the Mayer terms represent a terminal cost. A usual Lagrange objective function is to minimize the total amount of energy consumed during the maneuver. A typical Mayer objective function is to minimize the final time. Eq. (1b) and Eq. (1c) represent the differential-algebraic equation system that governs the motion of the dynamical system, e.g., the aircraft. Equation (1d) models the physical limits of performance of the dynamical system, typically expressed as upper and lower bounds on both states and control variables. Eq. (1e) and Eq. (1f) denote the boundary (initial and final, respectively) conditions of the process in which the system is involved. Note that Eq. (1c) and Eq. (1d) will also include the logical constraints that model storm avoidance and operational constraints as described in Section IV, which are the main interest of our study.

Hence, the optimal control problem (1a) - (1f) consists in finding an admissible control $u^*(t)$ such that the set of differential-algebraic subsystems follows an admissible trajectory $(x^*(t), u^*(t), s^*)$ between the initial and final state that minimizes the performance index $J(t, x(t), u(t), s, t)$. The final time, t_F, may be fixed or free.

C. Direct Collocation Transcription of the Optimal Control Problem

A direct numerical method has been employed to transcribe the OCP into a NLP problem. More specifically, a Hermite-Simpson direct collocation method [9] has been used. The time interval $[t_I, t_F]$ is subdivided into N subintervals of equal length Δt, whose endpoints are

$$\{t_0, t_1, \ldots, t_N\}, \tag{2}$$

with $t_0 = t_I$ and $t_N = t_F$. In each subinterval $[t_i, t_{i+1}]$, $i = 0, \ldots, N-1$, the Hermite-Simpson numerical integration scheme is used.

The set of constraints of the resulting NLP problem includes the Hermite-Simpson system constraints that correspond to the differential constraint (1b) and the discretized versions of the other constraints of the optimal control problem. They include the algebraic constraints (1c), the state and control envelope constraints (1d), and the boundary conditions (1e) and (1f). The unknowns of the NLP problem are the values of the state and the control variables at the endpoints of each subinterval $[t_i, t_{i+1}]$, $i = 0, \ldots, N-1$.

D. Closed-Loop Optimal Control

Following the idea depicted in Sect II-A and the open-loop model described in Sect II-B, the practical implementation of the closed-loop procedure can be summarized as follows:

(i) Consider de length interval Δt and the horizon length N, and let $k = 1$.
(ii) Solve the open-loop OPC (1a) - (1f) over the horizon $[t_{k-1}, t_{k-1} + N\Delta t]$ with initial state $x(t_{k-1})$ and obtain the control sequence $\{u(t_k), u(t_{k+1}), \ldots, u(t_{k+N})\}$.
(iii) Apply the control input $u(t_{k-1})$ for the time interval $[t_{k-1}, t_{k-1}+\Delta t]$ to the system in order to compute $x(t_k)$, and set $x(t_k)$ as the initial condition for the next iteration of the NMPC scheme.
(iv) Let $t_k = t_{k-1} + \Delta t$ and $k = k+1$, and repeat steps (ii) and (iii) until the target is reached.

As a consequence, the closed-loop procedure $(i) - (iv)$ provides a sequence of NLP problems. For this resulting series of NLP problems to be solved, the NLP interior point nonlinear solver IPOPT is one of the most suitable ones because it handles properly large-scale sparse nonconvex problems, with a large number of equality and inequality constraints. It implements an interior point line search filter method and can be used to solve general NLP problems. Moreover, it is open source. The mathematical details of the IPOPT algorithm can be found in [10]. Source and binary files are available at the Computational Infrastructure for Operations Research web site[2].

III. Aircraft Model Description

A. Equations of Motion

A common three-degree-of-freedom dynamic model has been used which describes the point variable-mass motion

[2]https://www.coin-or.org/

of the aircraft over an spherical Earth model. In particular, a symmetric flight has been considered. Thus, it has been assumed that there is no sideslip and all forces lie in the plane of symmetry of aircraft. The following equations of motion of the aircraft has been considered:

$$\begin{aligned}
\dot{V}(t) &= \frac{T(t) - D(h_e(t), V(t), C_L(t)) - m(t) \cdot g \cdot \sin\gamma(t)}{m(t)} \\
\dot{\chi}(t) &= \frac{L(h_e(t), V(t), C_L(t)) \cdot \sin\mu(t)}{m(t) \cdot V(t) \cdot \cos\gamma(t)} \\
\dot{\gamma}(t) &= \frac{L(h_e(t), V(t), C_L(t)) \cdot \cos\mu(t) - m(t) \cdot g \cdot \cos\gamma(t)}{m(t) \cdot V(t)} \\
\dot{\lambda_e}(t) &= \frac{V(t) \cdot \cos\gamma(t) \cdot \cos\chi(t) + V_{wind\lambda_e}}{R \cdot \cos\theta_e(t)} \\
\dot{\theta_e}(t) &= \frac{V(t) \cdot \cos\gamma(t) \cdot \sin\chi(t) + V_{wind\theta_e}}{R} \\
\dot{h_e}(t) &= V(t) \cdot \sin\gamma(t) \\
\dot{m}(t) &= -T(t) \cdot \eta(V(t))
\end{aligned} \tag{3}$$

The three dynamic equations in (3) are expressed in an aircraft-attached reference frame (x_w, y_w, z_w) and the three kinematic equations are expressed in a ground based reference frame (x_e, y_e, z_e).The states of the system (3) are $V, \chi, \gamma, \lambda_e, \theta_e, h_e$ and m. Thus, $x(t) = (V(t), \chi(t), \gamma(t), \lambda_e(t), \theta_e(t), h_e(t), m(t))$. State variables V, χ and γ refer to the true airspeed, heading angle, and flight path angle, respectively. State variables λ_e, θ_e and h_e refer to the aircraft three-dimensional (3D) position, longitude, latitude and altitude, respectively. The aircraft position in two dimensions (x_e, y_e) is approximated as $x_e = \lambda_e \cdot (R + h_e) \cdot \cos\theta_e$ and $y_e = \theta_e \cdot (R + h_e)$. Finally, state variable m refers to the aircraft mass. The controls inputs are the bank angle μ, the engine thrust T, and the lift coefficient C_L. Thus, $u(t) = (T(t), \mu(t), C_L(t))$. Parameter R is the radius of Earth, η is the speed-dependent fuel efficiency coefficient, and $V_{wind\lambda_e}$ and $V_{wind\theta_e}$ are de wind speed in the λ_e and θ_e components, respectively. Lift, $L = C_L S\hat{q}$, and drag, $D = C_D S\hat{q}$, are the components of the aerodynamic force. Parameter S is the reference wing surface area and $\hat{q} = \frac{1}{2}\rho V^2$ is the dynamic pressure. A parabolic drag polar $C_D = C_{D0} + KC_L^2$, and an International Standard Atmosphere (ISA) model are assumed. The lift coefficient C_L is a known function of the angle of attack α and the Mach number.

Note that differential equations in (3) take the form of (1b) of the continuous optimal control problem stated in Section II-B.

B. Flight Envelope Constraints

Flight envelope constraints are derived from the geometry of the aircraft, structural limitations, engine power, and aerodynamic characteristics. The performance limitations model and the parameters has been obtained from the Base of Aircraft Data (BADA), version 3.14 [11]:

$$\begin{aligned}
0 \le h_e(t) \le \min[h_{M0}, h_u(t)], \quad & \gamma_{min} \le \gamma(t) \le \gamma_{max}, \\
M(t) \le M_{M0}, \quad & m_{min} \le m(t) \le m_{max}, \\
\dot{V}(t) \le \bar{a}_l, \quad & C_v V_s(t) \le V(t) \le V_{Mo}, \\
\dot{\gamma}(t)V(t) \le \bar{a}_n, \quad & 0.1 \le C_L(t) \le C_{L_{max}}, \\
\mu(t) \le \bar{\mu}, \quad & T_{min}(t) \le T(t) \le T_{max}(t)
\end{aligned} \tag{4}$$

In (4), h_{M0} is the maximum reachable altitude and $h_u(t)$ is the maximum operative altitude at a given mass (it increases as fuel is burned). $M(t)$ is the Mach number and M_{M_0} is the maximum operating Mach number. C_v is the minimum speed coefficient, $V_s(t)$ is the stall speed, V_{M_0} is the maximum operating calibrated airspeed (CAS) and $\bar{a}_n$ and $\bar{a}_l$ are, respectively, the maximum normal and longitudinal accelerations for civilian aircraft. Finally, $T_{min}(t)$ and $T_{max}(t)$ correspond to the minimum and maximum available thrust, respectively, and $\bar{\mu}$ corresponds to the maximum bank angle due to structural limitations.

Note that inequality constraints in (4) take the form of (1d) of the continuous optimal control problem stated in Section II-B.

IV. Logical Constraints Modeling

In this section, the approach proposed in [12] has been followed, in which an extension of the embedding optimal control technique stated in [13] and developed in [14] has been proposed. The embedding technique has been introduced in [13], [14] to transform hybrid optimal control problems, in which the discrete aspect of the system arises from switches in the dynamic equations, into traditional smooth optimal control problems. It has been adapted in [12] to deal with logical (discrete) components which also might appear as constraints.

It has been shown in [15] that every Boolean expression can be transformed into Conjunctive Normal Form (CNF). Thus, it has been assumed that any logical constraint considered in this study can be written as a CNF expression

$$Q_1 \wedge Q_2 \wedge \ldots \wedge Q_n, \tag{5}$$

where

$$Q_i = P_i^1 \vee P_i^2 \vee \ldots \vee P_i^{m_i}. \tag{6}$$

Proposition P_i^j is either X_i^j or $\neg X_i^j$. Term X_i^j is a literal that can be either `True` or `False` and $\neg$ represents the negation or logical complement operator. Term X_i^j is used to represent statements such as "longitud $\lambda_e \le 40$". Therefore, P_i^j takes the form

$$P_i^j \equiv \{g_i^j(x(t)) \le 0\}, \tag{7}$$

where $g_i^j : \mathbb{R}^{n_x} \to \mathbb{R}$ is assumed to be a $\mathcal{C}^1$ function.

In order to include the logical constraint (5) into a smooth continuous optimal control problem formulation, it must be converted into a set of equality or inequality constraints in which binary variables are not considered. In this way, the combinatorial complexity of integer programming is avoided.

Transcribing the conjunction in (5) is straightforward since it is equivalent to the following expression

$$\forall i \in \{1, 2, \ldots, n\}: \quad D_i. \tag{8}$$

Thus, taking into account (6), the logical expression (5) can be represented as

$$\forall i \in \{1, 2, \ldots, n\}: \quad P_i^1 \vee P_i^2 \vee \ldots \vee P_i^{m_i}. \tag{9}$$

For the transcription of the disjunctions into a set of inequality constraints, a continuos variable $\beta_i^j \in [0, 1]$ is defined and related to each P_i^j in (7). Thus, (9) can be expressed as

$$\begin{aligned} \forall i \in \{1, 2, \ldots, n\}: \quad & \beta_i^j \cdot g_i^j(x(t)) \leq 0 \\ \text{and} \quad & 0 \leq \beta_i^j \leq 1 \\ \text{and} \quad & \sum_{j=1}^{m_i} \beta_i^j = 1. \end{aligned} \tag{10}$$

It is immediate to check that if $\beta_i^j = 0$ in the first term in (10), then constraint $g_i^j(x(t)) \leq 0$ is not fulfilled. On the contrary, if $0 < \beta_i^j \leq 1$ then $\beta_i^j \cdot g_i^j(x(t)) \leq 0$ is in fact $g_i^j(x(t)) \leq 0$, and thus constraint $g_i^j(x(t)) \leq 0$ is enforced. Finally, the last term in (10) guarantees that at least one of the propositions P_i^j holds.

Note that, as expected, equality and inequality constraints in (10) take the form of (1c) and (1d), respectively, of the traditional open-loop continuous optimal control problem stated in Section II-B. In the following subsections, the application of this technique to storm avoidance and aircraft flying through waypoints modelling will be presented in detail.

A. Storm Avoidance Constraint

The model of the cells of the storm has been based on the use of ellipsoids. More specifically, each cell of the storm has been modelled as a moving obstacle in the 3D space enveloped by an ellipsoid. This simple approach allows us to specify each cell by giving only the coordinates of one moving point in the three dimensional environment. In this way, the storm avoidance problem is tackled like an obstacle avoidance problem, in which for each aircraft a safety distance-based separation between each aircraft and the centre point of the cell is guaranteed in the horizontal or vertical directions.

Let $(\lambda_i, \theta_i, h_i)$ and $(\lambda_{C_i}, \theta_{C_i}, h_{C_i})$ be the positions of a single aircraft and the centre point of cell C at the endpoint t_i of the discretization, respectively. Let the safety distance-based separation in the $\lambda - \theta$ and h directions at every endpoint t_i be denoted by $d_{\lambda\theta_i}$ and d_{h_i}, respectively. Note that changing the size of safety distances $d_{\lambda\theta_i}$ and d_{h_i} allows size-changing cells to be modelled. Then, the storm avoidance constraints can be expressed as

$$\begin{aligned} \forall i \in \{1, 2, \ldots, N\}: \quad & 2R \operatorname{atan2}\left(\sqrt{\zeta_i}, \sqrt{1-\zeta_i}\right) \geq d_{\lambda\theta_i} \\ \text{or} \quad & |h_i - h_{C_i}| \geq d_{h_i}, \end{aligned} \tag{11}$$

where the haversine formula has been consider for the distance in the $\lambda - \theta$ direction with

$$\zeta_i = \sin^2\left(\frac{\theta_i - \theta_{C_i}}{2}\right) + \cos\theta_i \cos\theta_{C_i} \sin^2\left(\frac{\lambda_i - \lambda_{C_i}}{2}\right).$$

The set of constraints (11) can be rewritten as

$$\begin{aligned} \forall i \in \{1, 2, \ldots, N\}: \quad & 2R \operatorname{atan2}\left(\sqrt{\zeta_i}, \sqrt{1-\zeta_i}\right) \geq d_{\lambda\theta_i} \\ \text{or} \quad & h_i - h_{C_i} \geq d_{h_i}. \end{aligned} \tag{12}$$

Following the technique described above, new variables $\nu_i^j \in [0, 1]$ for $i = 1, 2, \ldots, N, j = 1, 2$ satisfying condition

$$\sum_{j=1}^{2} \nu_i^j = 1$$

are introduced, and Eq. (12) can be transformed into

$$\begin{aligned} & \forall i \in \{1, 2, \ldots, N\}: \\ & \nu_i^1 \left(2R \operatorname{atan2}\left(\sqrt{\zeta_i}, \sqrt{1-\zeta_i}\right) - d_{\lambda\theta_i}\right) \geq 0 \\ \text{and} \quad & \nu_i^2 (h_i - h_{C_i} - d_{h_i}) \geq 0 \\ \text{and} \quad & 0 \leq \nu_i^j \leq 1, j = 1, 2 \\ \text{and} \quad & \sum_{j=1}^{2} \nu_i^j = 1. \end{aligned} \tag{13}$$

The last constraint in (13) ensures that at least one of the constraints in (12) is fulfilled, that is, the aircraft and the storm are guaranteed to be a safe distance apart. Moreover, since this embedded logical constraint approach is quite general, any other storm avoidance model described in terms of Eq. (6) can be considered.

B. Waypoint Constraints

The design of the waypoints has been based on the use of cuboids. More specifically, a cuboid centered at each waypoint has been defined, in such a way that passage constrains through waypoints have been modeled as passage constrains through cuboids.

Let $(\lambda_{W_l}, \theta_{W_l}, h_{W_l})$ and $(\lambda_{W_u}, \theta_{W_u}, h_{W_u})$ be the positions of opposite corners of a cuboid surrounding a single waypoint. Flying by this waypoint (that is, passing through the corresponding cuboid) involves that at every endpoint t_i of the subintervals of the discretization (2), the position of the aircraft $(\lambda_i, \theta_i, h_i)$ must remain inside it. In terms of logical constraints, this condition can be expressed as

$$\begin{aligned} \forall i \in \{1, 2, \ldots, N-1\}: \quad & \lambda_{W_l} - \lambda_i \leq 0 \\ \text{and} \quad & \lambda_i - \lambda_{W_u} \leq 0 \\ \text{and} \quad & \theta_{W_l} - \theta_i \leq 0 \\ \text{and} \quad & \theta_i - \theta_{W_u} \leq 0 \\ \text{and} \quad & h_{W_l} - h_i \leq 0 \\ \text{and} \quad & h_i - h_{W_u} \leq 0. \end{aligned} \tag{14}$$

Note that, on the one hand, constraints (14) are enforced at every point of the discretization except for the initial and final points, t_0 and t_N, since there is no a priori knowledge about when the aircraft is going to fly by the waypoint. On the other hand, these constraints obviously make sense only when the aircraft is closed enough to the waypoint.

To overcome this drawback a second auxiliary cuboid is considered to modelled freeflight mode of the aircraft. Let

$\lambda_{min}, \theta_{min}, h_{min}, \lambda_{max}, \theta_{max}$ and h_{max} be the minimum and maximum values of the state variables λ, θ and h, respectively. In terms of logical constraints, the freeflight mode condition can be expressed as

$$\begin{aligned} \forall i \in \{1, 2, \ldots, N-1\}: \quad & \lambda_{min} - \lambda_i \leq 0 \\ \text{and} \quad & \lambda_i - \lambda_{max} \leq 0 \\ \text{and} \quad & \theta_{min} - \theta_i \leq 0 \\ \text{and} \quad & \theta_i - \theta_{max} \leq 0 \\ \text{and} \quad & h_{min} - h_i \leq 0 \\ \text{and} \quad & h_i - h_{max} \leq 0. \end{aligned} \tag{15}$$

Then, the transcription into a logical disjunction to select along the whole trajectory between flying by the Waypoint Mode (WM) or Freeflight Mode (FM), namely WM $\vee$ FM, can be expressed as

$$\begin{aligned} \forall i \in \{1, 2, \ldots, N-1\}: \quad & \mathsf{WM}_i \\ \text{or} \quad & \mathsf{FM}_i, \end{aligned} \tag{16}$$

where WM_i and FM_i denote if at discretization instant i the aircraft is in waypoint mode or freeflight mode, respectively.

Once again, following the technique described above, if we define new variables $\kappa_i^1, \kappa_i^2 \in [0, 1]$ satisfying condition

$$\kappa_i^1 + \kappa_i^2 = 1, \quad \text{for all} \quad i = 1, 2, \ldots, N-1,$$

Eq. (16) can be transformed into

$$\begin{aligned} & \forall i \in \{1, 2, \ldots, N-1\}: \\ & \kappa_i^1(\lambda_{W_l} - \lambda_i) \leq 0 \quad \text{and} \quad \kappa_i^2(\lambda_{min} - \lambda_i) \leq 0 \\ \text{and} \quad & \kappa_i^1(\lambda_i - \lambda_{W_u}) \leq 0 \quad \text{and} \quad \kappa_i^2(\lambda_i - \lambda_{max}) \leq 0 \\ \text{and} \quad & \kappa_i^1(\theta_{W_l} - \theta_i) \leq 0 \quad \text{and} \quad \kappa_i^2(\theta_{min} - \theta_i) \leq 0 \\ \text{and} \quad & \kappa_i^1(\theta_i - \theta_{W_u}) \leq 0 \quad \text{and} \quad \kappa_i^2(\theta_i - \theta_{max}) \leq 0 \\ \text{and} \quad & \kappa_i^1(h_{W_l} - h_i) \leq 0 \quad \text{and} \quad \kappa_i^2(h_{min} - h_i) \leq 0 \\ \text{and} \quad & \kappa_i^1(h_i - h_{W_u}) \leq 0 \quad \text{and} \quad \kappa_i^2(h_i - h_{max}) \leq 0 \\ \text{and} \quad & 0 \leq \kappa_i^j \leq 1, j = 1, 2 \\ \text{and} \quad & \sum_{j=1}^{2} \kappa_i^j = 1. \end{aligned} \tag{17}$$

The last constraint in (17) ensures that at least one of the conditions in (16) is fulfilled, which means that at each discretization instant i the aircraft flies in freeflight mode or waypoint mode. Note that, depending on the performance index (1a) considered in the optimal control problem, two related undesired issues could potentially arise.

On the one hand, the optimal solution could provide a trajectory in which the aircraft flies in freeflight mode for each discretization instant i. Therefore, in order to force the aircraft to actually fly by the waypoint, a penalization term must also be added to the numerical transcription of the performance index (1a). The use of this penalization term, which is set forth to encode the desired control objectives, implies that the numerical solution of the optimal control problem must combine the usual collocation technique describe in Section II-C with a penalty function methodology. In particular, in this work, the well-known continuation method has been implemented following a similar approach to [16]. For waypoint modeling the penalization term takes the form

$$c_1 \sum_{i=1}^{N-1} \kappa_i^1 + c_2 \sum_{i=1}^{N-1} \kappa_i^2, \tag{18}$$

where c_1 and c_2 are suitable constants determined by the continuation method. In the case of the minimization of a performance index like (1a), a large enough value c_2 such that $c_2 \gg c_1 > 0$, which penalizes the freeflight mode, guarantees that the aircraft actually flies by the waypoint.

On the other hand, the optimal solution could provide a trajectory in which the aircraft flies by the waypoint more than once. This situation can be easily avoided introducing in the model the following simple constraint

$$\sum_{i=1}^{N-1} \kappa_i^1 \leq c_3, \tag{19}$$

where $c_3 \in \{1, 2, \ldots, N-1\}$ is a suitable constant. In the context of the problem considered in this work, to include the penalty term (18) in the objective functional, a small value of c_3 is enough to avoid this potential undesired issue.

Note that the waypoint constraint modelling introduced above can be straightforwardly extended to multi-waypoint and multi-aircraft cases. Moreover, since the employed logical constraint modelling technique is quite general, any other waypoint constraint described in terms of Eq. (6) can be modeled.

V. Numerical Results

To show the effectiveness of the methodology described in Section IV, a numerical experiment has been carried out. In particular, the minimum-time STAR-based CDO of three aircraft along converging routes has been studied. Following this STAR procedure, in principle, the three aircraft are assumed to pass through two waypoints. However, the experiment has been intentionally designed in such a way that a cell of the storm also passes through the second waypoint when an aircraft is approaching it. A decision making process has been devised which attending to safety reasons, in case of temporal coincidence between a cell of the storm and an aircraft at a waypoint, avoiding the cell of the storm is assumed to be preferable than crossing the waypoint.

The numerical experiment involves Airbus A-320 BADA 3.14 aircraft models, in which the performance index is the sum of the duration of the flights of the three aircraft. A constant crosswind has been considered along with a multi-cell storm in development whose cells grow in dimension, move, split and merge.

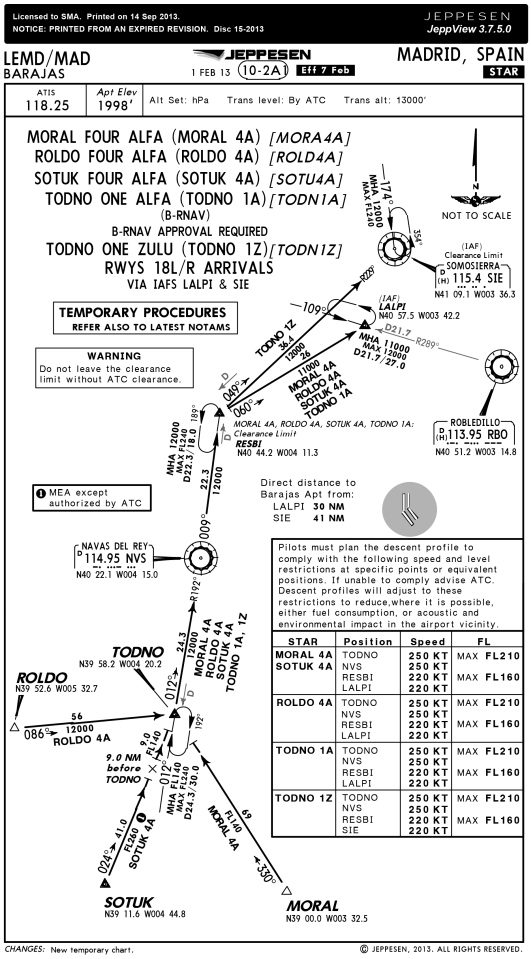

Fig. 1. Chart of the Adolfo Suárez Madrid-Barajas (LEMD/MAD) STAR 10-2A1 printed from JEPPESEN.

TABLE I
BOUNDARY CONDITIONS FOR THE STAR BASED CDO

Symbol	Unit	Aircraft 1	Aircraft 2	Aircraft 3
h_I	m	7400	7000	7200
h_F	m	3350	3350	3350
θ_I	deg	39.526	39.116	39.000
θ_F	deg	40.575	40.575	40.575
λ_I	deg	-5.327	-4.448	-3.325
λ_F	deg	-3.422	-3.422	-3.422
V_I	m/s	130	130	130
V_F	m/s	110	110	110
μ_I	deg	0	0	0
γ_I	deg	0	0	0
χ_I	deg	356	294	240
m_I	kg	65000	65000	65000

In the proposed STAR procedure, the lateral path followed by the aircraft has been assumed to be specified in a navigation chart. In particular, the boundary conditions of the state variables have been selected from the chart of the Adolfo Suárez Madrid-Barajas (LEMD/MAD) TMA shown in Fig. 1. The initial position of Aircraft 1, Aircraft 2, and Aircraft 3 are supposed to be coincident with the ROLDO, SOTUK and MORAL waypoints, respectively. Aircraft are constrained to pass through TODNO and RESBI waypoints and their common final position is assumed to be the LALPI waypoint. For the setting of the cuboids centered at the given waypoints the modeling technique defined in (14) has been used. In particular, the cuboid centered at TODNO waypoint has been defined by the two corners $(39.560°, -4.24°, 5400 \text{ m})$ and $(39.640°, -4.160°, 6000 \text{ m})$ whereas the cuboid centered at RESBI waypoint has been defined by the two corners $(40.400°, -4.150°, 4200 \text{ m})$ and $(40.480°, -4.070°, 4800 \text{ m})$.

A constant crosswind of 30 m/s westbound has been considered together with a multi-cell storm in development as shown in 2 and 3. Cell 1 grows in dimension and moves straight in the same direction as the wind but with a constant speed of 18.5 m/s without splitting. Cell 2 is the result of merging of two other cells. It grows in dimension and moves first straight in the same direction as the wind and then it changes direction. Cell 3 grows in dimension and moves straight in the same direction as the wind but with a constant speed of 18.5 m/s splitting in two different cells which move in different directions. Moreover, Cell 2 passes through the RESBI waypoint from right side to left side in steady level. The experiment has been designed in such a way that there is a potential interference between a cell of the storm and the aircraft at RESBI waypoint. Cells have been modelled as a growing ellipsoids, as explained in Section IV-A. In general, the cell growth can be modeled by increasing both the safety distances $d_{\lambda\theta_i}$ and d_{h_i}. In this specific experiment, only in the $d_{\lambda\theta_i}$ distance has been increased from 7000 m to 10000 m.

The initial mass of the three aircraft has been assumed equal to the maximum landing weight of the aircraft. The specific boundary conditions of the aircraft state variables are given in Table I.

In Fig. 2, the 3D view of the paths obtained in the solution are represented in thin lines whereas in Fig. 3 and Fig. 4 the horizontal and vertical profiles are represented.

The mass consumption is represented in Fig. 5, in which the solution with waypoint and storm avoid constraints is represented. The final mass and time given by the solution of the corresponding OCP are reported for each aircraft in the second row of Table II.

In principle, the three aircraft are assumed to pass through both waypoints and, at the same time, they must avoid the storm. However, as it can be seen in Fig. 2, only the aircraft coming from MORAL waypoint is able to avoid the storm and reach both waypoints TODNO and RESBI. The other two aircraft also avoid the storm but they only reach the TODNO waypoint. This is due to the fact that the performance index includes in this case, besides the minimization of the duration of the flights, a penalization term associated to the waypoints constraints in such a way that, as explained above, the storm constraint is always preferable for safety reasons.

TABLE II
RESULTS OF STAR BASED CDO WITH WAYPOINT AND STORM AVOID CONSTRAINTS

Aircraft origin	Final time, s	Final mass, kg
ROLDO	1941	63888
SOTUK	1742	64003
MORAL	2382	63638

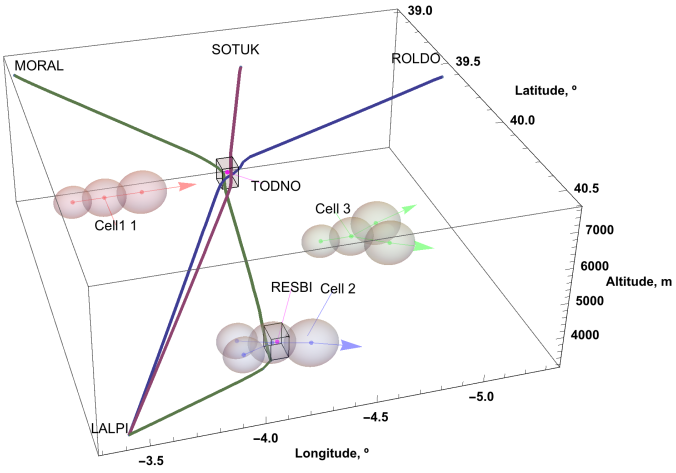

Fig. 2. 3D view of the aircraft trajectories with waypoint and storm avoidance constraints.

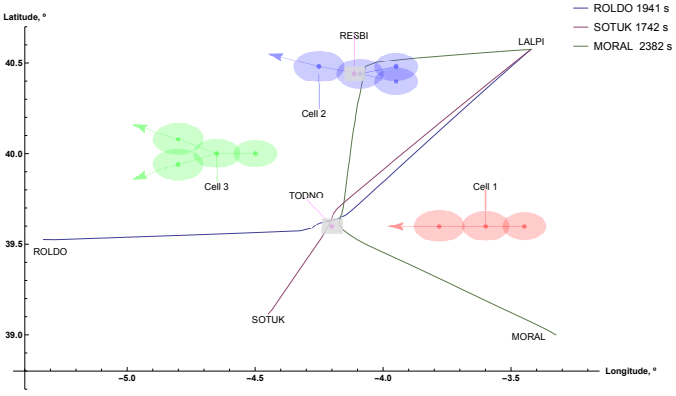

Fig. 3. Horizontal profile of the aircraft trajectories with waypoint and storm avoidance constraints.

VI. CONCLUSIONS

In this paper, the trajectory generation problem has been studied for multiple aircraft in converging and intersecting arrival routes within the Adolfo Suárez Madrid-Barajas (LEMD/MAD) TMA in the presence of a multi-cell storm in development. The storm avoidance constraints have been enforced by approximating the cells of the storm as moving and size-changing ellipsoids, and the resulting problem has been solved by using nonlinear model predictive control based on hybrid optimal control with logical constraints in disjunctive form. The logical constraints in disjunctive form have been transformed into inequality and equality constraints which

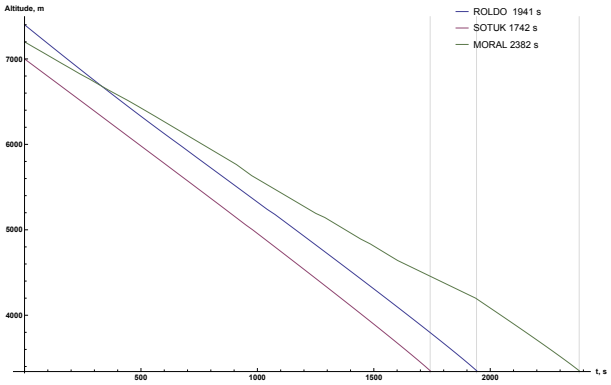

Fig. 4. Vertical profile of the aircraft trajectories with waypoint and storm avoidance constraints.

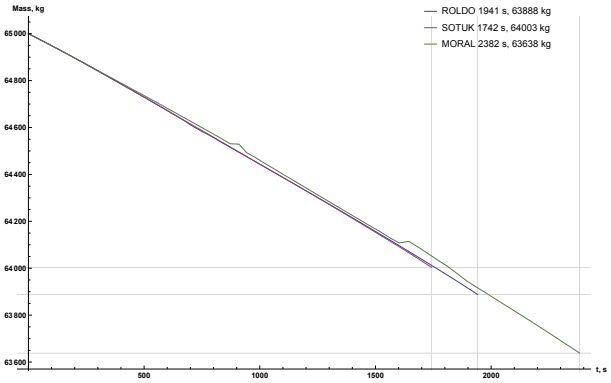

Fig. 5. Mass consumption the aircraft trajectories with waypoint and storm avoidance constraints.

involves only continuous auxiliary variables. In this way, the optimal control problem with logical constraints has been converted into a smooth optimal control problem which has been solved using standard techniques. The numerical results show the effectiveness of the proposed technique.

REFERENCES

[1] L. Grüne and J. Pannek, *Nonlinear Model Predictive Control*. Springer, 2011.

[2] International Civil Aviation Organization, "Continuous Descent Operations (CDO) Manual, Document 9931," tech. rep., ICAO, 2010.

[3] E. Itoh, M. Brown, A. Senoguchi, N. Wickramasinghe, and S. Fukushima, "Future arrival management collaborating with trajectory-based operations," in *Air Traffic Management and Systems II. Lecture Notes in Electrical Engineering, vol. 420* (Electronic Navigation Research Institute, ed.), pp. 137–156, Springer, 2017.

[4] J. Pannequin, A. Bayen, I. Mitchell, H. Chung, and S. Sastry, "Multiple aircraft deconflicted path planning with weather avoidance constraints," in *Proceedings of the AIAA Guidance, Navigation and Control Conference and Exhibit*, (Hilton Head, SC, USA), 2007.

[5] M. Kamgarpour, V. Dadok, and C. Tomlin, "Trajectory generation for aircraft subject to dynamic weather uncertainty," in *Proceedings of the 49th IEEE Conference on Decision and Control*, (Atlanta, GA, USA), 2010.

[6] S. Summers, M. Kamgarpour, C. Tomlin, and J. Lygeros, "A stochastic reach-avoid problem with random obstacles," in *Proceedings of the 14th ACM International Conference on Hybrid Systems: Computation and Control*, (Chicago, IL, USA), 2011.

[7] D. Hentzen, M. Kamgarpour, M. Soler, and D. González-Arribas, "On maximizing safety in stochastic aircraft trajectory planning with uncertain thunderstorm development," *Aerospace Science and Technology*, vol. 79, pp. 543–553, 2018.
[8] B. Zhang, L. Tang, and M. Roemer, "Probabilistic planning and risk evaluation based on ensemble weather forecasting," *IEEE Transactions on Automation Science and Engineering*, vol. 15, no. 2, pp. 556–566, 2018.
[9] C. R. Hargraves and S. W. Pairs, "Direct trajectory optimization using nonlinear programming and collocation," *Journal of Guidance, Control, and Dynamics*, vol. 10, no. 4, pp. 338–342, 1987.
[10] A. Wachter and L. Biegler, "On the implementation of an interior-point filter line-search algorithm for large-scale nonlinear programming," *Mathematical Programming*, vol. 106, no. 1, pp. 25–57, 2006.
[11] V. Mouillet, "User Manual for the Base of Aircraft Data (BADA) Revision 3.14," tech. rep., EUROCONTROL Experimental Centre, Brétigny, France, 2017.
[12] S. Wei, M. Zěfran, and R. A. DeCarlo, "Optimal control of robotic systems with logical constraints: Application to UAV path planning," in *Proceedings of the 2008 IEEE International Conference on Robotics and Automation*, (Pasadena, CA, USA), 2008.
[13] S. C. Bengea and R. A. DeCarlo, "Optimal control of switching systems," *Automatica*, vol. 41, pp. 11–27, 2005.
[14] S. Wei, K. Uthaichana, M. Zefran, R. A. DeCarlo, and S. Bengea, "Applications of numerical optimal control to non-linear hybrid systems," *Nonlinear Analysis: Hybrid Systems*, vol. 1, no. 2, pp. 264–279, 2007.
[15] T. M. Cavalier, P. M. Pardalos, and A. L. Soyster, "Modeling and integer programming techniques applied to propositional calculus," *Computers and Operations Research*, vol. 17, no. 6, pp. 561–570, 1990.
[16] S. Wei, K. Uthaichana, M. Zefran, and R. A. DeCarlo, "Hybrid model predictive control for the stabilization of wheeled mobile robots subject to wheel slippage," *IEEE Transactions on Control Systems Technology*, vol. 21, pp. 2181–2193, 2013.

Dinesh B. Seenivasan is a PhD student at the Universidad Rey Juan Carlos in Madrid, Spain. He received his BSc in Aeronautical Engineering from the Anna University of Chennai, India, and his MSc in Aerospace Engineering from the Universidad Politécnica de Madrid. His research interests include stochastic hybrid optimal control and model predictive control with applications to aeronautics.

Alberto Olivares is a Professor of Statistics and Vector Calculus at the Universidad Rey Juan Carlos in Madrid, Spain. He received his MSc in Mathematics and his BSc in Statistics from the Universidad de Salamanca, Spain, and his PhD degree in Mathematical Engineering from the Universidad Rey Juan Carlos. He worked with the Athens University of Economics and Business. His research interests include statistical learning, stochastic hybrid optimal control and model predictive control with applications to biomedicine, robotics, aeronautics and astronautics.

Ernesto Staffetti is a Professor of Statistics and Control Systems at the Universidad Rey Juan Carlos in Madrid, Spain. He received his MSc in Automation Engineering from the Università degli Studi di Roma "La Sapienza," and his PhD degree in Advanced Automation Engineering from the Universitat Politècnica de Catalunya. He worked with the Universitat Politècnica de Catalunya, the Katholieke Universiteit Leuven, the Spanish Consejo Superior de Investigaciones Científicas, and with the University of North Carolina at Charlotte. His research interests include stochastic hybrid optimal control, iterative learning control and model predictive control with applications to robotics, aeronautics and astronautics.